Accurate Born-Oppenheimer potentials for excited Σ^+ states of the hydrogen molecule

Michał Siłkowski*, Magdalena Zientkiewicz, Krzysztof Pachucki

Faculty of Physics, University of Warsaw, Pasteura 5, 02-093 Warsaw, Poland

Abstract

We report on highly accurate calculations of Born-Oppenheimer potentials for excited $n\,\Sigma^+$ states of the hydrogen molecule for all possible combinations of singlet/triplet and gerade/ungerade symmetries up to $n = 7$. A relative accuracy of 10^{-10} (0.00002 cm^{-1}) or better is achieved for all the internuclear distances and all the excited states under consideration – an improvement with respect to the best results available in the literature by at least 6 orders of magnitude. Presented variational calculations rely on efficient evaluation of molecular integrals with the explicitly correlated exponential basis in arbitrary precision arithmetics.

Keywords: hydrogen molecule, excited states, Born-Oppenheimer potential, explicitly correlated methods
PACS: 31.15.ac, 31.15.vn, 31.50.Df

1. Introduction

Ab initio Born-Oppenheimer potentials have proven to be invaluable for the interpretation of spectroscopic data. Currently, transitions between rovibrational levels of $X\,^1\Sigma_g^+$ ground state for hydrogen molecule isotopologues are a subject of exhaustive investigations both from experimental [1, 2, 3] and theoretical [4, 5] standpoints, reaching the accuracy of 10^{-4} cm^{-1}. On the contrary, electronically excited states of the hydrogen molecule are much less studied, especially by theoretical methods. So far, calculations of Born-Oppenheimer (BO) potentials for excited Σ^+ states of

*Corresponding author
Email address: michal.silkowski@fuw.edu.pl (Michał Siłkowski)

H_2 were performed with full CI method [6, 7, 8], variational calculations with generalized GTOs [9], variational calculations with explicitly correlated gaussians (ECG) [10, 11] and more recently with free-complement local-Schrödinger-equation method (FC-LSE) [12]. The most accurate to date are variational calculations in an explicitly correlated exponential basis by Wolniewicz and co-workers [13, 14, 15, 16, 17] and by Komasa *et al.* [10, 11] which, remarkably have remained unsurpassed for the last 20 years.

Among the plethora of H_2 excited states, of particular importance and long-standing interest is the $B\,^1\Sigma_u^+$ state, the lowest of $^1\Sigma_u^+$ symmetry. It is easily accessible for spectroscopic measurements, through the allowed electric dipole transition from the $X\,^1\Sigma_g^+$ ground state, therefore, it can be measured very accurately and serve as a calibration marker at XUV frequencies. Likewise, energies of states such as $EF\,^1\Sigma_g^+$, $GK\,^1\Sigma_g^+$, $B\,^1\Sigma_u^+$ and $B'\,^1\Sigma_u^+$ are of great spectroscopic interest, because they comprise intermediate states in multiphoton processes, which are crucial for investigations of doubly excited states, recognized as resonant states involved in the dynamics of preionization and predissociation [18, 19, 20].

Moreover, BO potentials comprise an essential input for Multichannel Quantum Defect theory analyses of Rydberg states, where an accuracy of BO energies better than $0.001\,\mathrm{cm}^{-1}$ is required [21, 22], especially for the highly excited states, despite their minor spectroscopic relevance due to their experimental inaccessibility from the ground state. Accurate potentials are also important for studying *gerade/ungerade* mixing effects [23] beyond the BO approximation. Ultimately, accurate BO potentials may serve as a useful benchmark for less precise computational methods, electron-ion scattering experiments and numerous other applications [24, 25, 26]. We note that many previous calculations often come without estimation of uncertainties, making definitive comparisons rather difficult.

2. Method

The variational BO potentials reported in this work are obtained with the use of explicitly correlated exponential functions [27] of the form,

$$\Psi_\Sigma = \sum_{\{n\}} c_{\{n\}}\,(1 \pm P_{AB})\,(1 \pm P_{12})\,\Phi_{\{n\}}, \tag{1}$$

where P_{AB} permutes the nuclei A and B, P_{12} interchanges the two electrons and appropriate $\pm$ signs are chosen to fulfil the symmetry criteria for

gerade/ungerade and *singlet/triplet* states. Linear coefficients $c_{\{n\}}$ form an eigenvector, which is a solution of a secular equation. Trial wavefunctions $\Phi_{\{n\}}$ are given by,

$$\Phi_{\{n\}} \;=\; e^{-y\,\eta_1 - x\,\eta_2 - u\,\xi_1 - w\,\xi_2} r_{12}^{n_0}\, \eta_1^{n_1}\, \eta_2^{n_2}\, \xi_1^{n_3}\, \xi_2^{n_4}, \tag{2}$$

where η_i and ξ_i are proportional to confocal elliptic coordinates and are given by $\eta_i = r_{iA} - r_{iB}$, $\xi_i = r_{iA} + r_{iB}$, y, x, u and w are real, nonlinear parameters subject to variational minimization. The index $\{n\}$ denotes $\{n\} = (n_0, n_1, n_2, n_3, n_4)$ and enumerates all powers of coordinates allowed by symmetry restrictions, with an additional constraint,

$$\sum_{j=0}^{4} n_j \leq \Omega, \tag{3}$$

which determines the total size of the basis, once Ω is set. Analogously to the Hylleraas basis, a trial wavefunction is uniquely characterized by the set of $\{n\}$ and nonlinear parameters, which are common to all trial functions within a given sector.

In this work we use two sectors, each with its own nonlinear parameters, and with no additional symmetry restrictions. With Ω determining the total size of the first sector, the second sector's principal number is chosen as $\Omega - 2$, a heurestic optimum for most cases. In previous works [29, 30] concerning ground $X\,{}^1\Sigma_g^+$ or $b\,{}^3\Sigma_u^+$ states the James-Coolidge ($x = y = 0$) or generalized Heitler-London ($x = -y, u = w$) was utilized. The reasoning behind the more general basis used in this work stems from a fairly universal trend of wavefunctions being composed predominantly of $(1s, n'l)$ configurations with high values of n' and l [6, 7, 8, 31], where in the language of atomic orbitals, one electron is highly excited. This implies substantial asymmetry, $x \neq y$ and $u \neq w$, and demands a more flexible basis to accurately represent the wavefunction. In addition, the contribution of ionic configuration $(1s', 1s')$ grows more significant not only for singlet [16, 6, 7] but also for triplet symmetry [8], and there are states in the ${}^1\Sigma^+$ manifolds where it is essential [28] for significantly broad ranges of internuclear distances.

Thirdly, in contrast to the $X\,1\Sigma_g^+$ and $b\,{}^3\Sigma_u^+$ states, BO potentials for higher n exhibit much more complicated structure – a result of mutual avoided crossings and resonant interaction with the H^+H^- configurations, often resulting in double minima or bumps, rather than a smooth, single

minimum Morse-like curve. This, in turn, implies the presence of strong configuration mixing in some regions of R, unlike the case of well-separated $X\,^1\Sigma_g^+$ and $b\,^3\Sigma_u^+$ states.

Justification for introducing a second sector into the basis set follows from the presence of distinct scales of motion, namely, around the nuclei and another for larger distances [32, 33]. Many previous calculations utilize specific structure of the basis, tailored for a single state or symmetry, often with *a priori* knowledge about the chemical bond character or atomic orbitals approximation. Here, we emphasize the universality of our approach – nonlinear parameters for both sectors are thoroughly optimized in an unrestricted Kolos-Wolniewicz basis [28, 34] separately for each state and every internuclear distance. This basis is capable of accurately representing ionic and covalent structure with correct long-range asymptotics and short-range vicinities of interparticle cusps, as well as complicated radial nodes, which are expected in highly excited states.

A crucial point of our computational method is that it relies on the fact that all the necessary matrix elements of the nonrelativistic Hamiltonian,

$$H = -\frac{\nabla_1^2}{2} - \frac{\nabla_2^2}{2} - \frac{1}{r_{1A}} - \frac{1}{r_{1B}} - \frac{1}{r_{2A}} - \frac{1}{r_{2B}} + \frac{1}{r_{12}} + \frac{1}{r_{AB}}, \tag{4}$$

can be readily constructed as a linear combination of f-integrals, which are given by differentiation with respect to the corresponding nonlinear parameter, with $r = r_{AB}$,

$$f(r, n_0, n_1, n_2, n_3, n_4) = \frac{(-1)^{n_0+n_1+n_2+n_3+n_4}}{n_0!\, n_1!\, n_2!\, n_3!\, n_4!} \frac{\partial^{n_0}}{\partial w_1^{n_0}}\bigg|_{w_1=0} \frac{\partial^{n_1}}{\partial y^{n_1}} \frac{\partial^{n_2}}{\partial x^{n_2}} \frac{\partial^{n_3}}{\partial u^{n_3}} \frac{\partial^{n_4}}{\partial w^{n_4}} f(r)\,, \tag{5}$$

of $f(r)$, called the master integral [27],

$$f(r) = r \int \frac{d^3 r_1}{4\,\pi} \int \frac{d^3 r_2}{4\,\pi} \frac{e^{-w_1\, r_{12} - u\,(r_{1A}+r_{1B}) - w\,(r_{2A}+r_{2B}) - y\,(r_{1A}-r_{1B}) - x\,(r_{2A}-r_{2B})}}{r_{12}\, r_{1A}\, r_{1B}\, r_{2A}\, r_{2B}}. \tag{6}$$

The master integral (6) satisfies the differential equation [35, 36],

$$\left[\sigma_4 \frac{d^2}{d\,r^2}\, r\, \frac{d^2}{d\,r^2} + \sigma_2 \frac{d}{d\,r}\, r\, \frac{d}{d\,r} + \sigma_0\, r\right] f(r) = F(r), \tag{7}$$

where

$$\begin{aligned}
\sigma_0 &= w_1^2\,(u+w-x-y)\,(u-w+x-y)\,(u-w-x+y)\,(u+w+x+y) \\
&\quad +16\,(w\,x-u\,y)\,(u\,x-w\,y)\,(u\,w-x\,y), \\
\sigma_2 &= w_1^4-2\,w_1^2\,(u^2+w^2+x^2+y^2)+16\,u\,w\,x\,y, \\
\sigma_4 &= w_1^2\,,
\end{aligned} \tag{8}$$

and $F(r)$ is an inhomogeneous term, which involves exponential functions, exponential integral functions Ei, and the natural logarithm, with nonlinear parameters as their arguments, see Eq. (7) of Ref. [27] for explicit expression.

The differential equation (7) entails that the master integral $f(r)$ and all its derivatives with respect to nonlinear parameters have a Taylor-like expansion in r,

$$f(r)=\sum_{n=1}^{\infty}\left[f_n^{(1)}\,(\ln(r)+\gamma_{\rm E})+f_n^{(2)}\right]r^n\,, \tag{9}$$

where $\gamma_{\rm E}$ is the Euler-Mascheroni constant. Derivation of efficient recursion relations for evaluation of coefficients $f_n^{(1)}$ and $f_n^{(2)}$ constitutes an essential step towards evaluating f-integrals with arbitrary y, x, u and w nonlinear parameters and arbitrary precision, see Ref. [27] for more details.

Once all matrix elements are constructed in terms of f-integrals, the electronic energy is found as the nth lowest eigenvalue by refining an initial guess with inverse iteration method. This step is the most time consuming part of our computational method, because it scales as $\mathcal{O}(N^3)$, where N is the total size of the basis. Recently, interest in Aasen's algorithm [37] for indefinite matrix factorization has been revived due to a novel communication-avoiding variant [38], suitable for efficient parallelization on modern computer architectures.

In our calculations a custom implementation of this algorithm inspired by the PLASMA library [39] was utilized with custom vectorization of quad-double arithmetics based on Bailey's quad-double precision algorithms [40]. Incorporation of both the communication-avoiding variant of Aasen's factorization and vectorized quad-double arithmetics constitutes a very efficient implementation of dense matrix factorization – an essential component of the inverse iteration method with nonorthogonal bases. Extension to octuple precision arithmetics has proven sufficient to contend with near-singular matrices, ill-conditioning of which can be attributed to the presence of large powers of the r_{12} coordinate in the basis.

3. Results and discussion

Reported BO energies are calculated for all possible symmetries of the Σ^+ manifold: $n^1\Sigma_g^+$, $n^3\Sigma_g^+$, $n^1\Sigma_u^+$, and $n^3\Sigma_u^+$, with $n \leq 7$ (26 states in total), with the exception of the ground $X\,^1\Sigma_g^+$ and $b\,^3\Sigma_u^+$ states, which were calculated elsewhere [29, 30] using special cases of the KW basis. The results are obtained on a grid of internuclear distances resembling logarithmic spacing in the range $R = 0.7 - 20.0$ au (72 points per state in total). It is sampled with denser spacing of 0.1 au in the region of $R = 4.0 - 6.0$ au, where potential curves demonstrate strong avoided crossing features and are subject to rapid changes as a function of R.

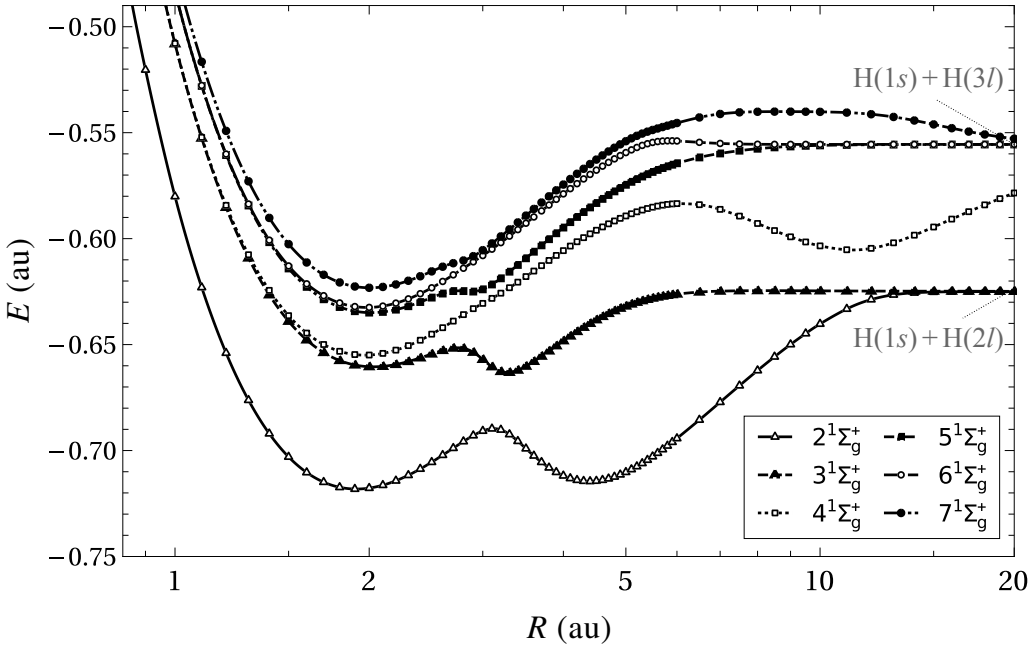

Figure 1: BO potentials for $n^1\Sigma_g^+$ states, up to $n = 7$. In this scale the $X\,1^1\Sigma_g^+$ ground state is not visible. The $GK\,3^1\Sigma_g^+$ with $H\,4^1\Sigma_g^+$ and $P\,5^1\Sigma_g^+$ with $O\,6^1\Sigma_g^+$ switch character from united atom $3d\sigma$ and $4d\sigma$ configurations to $3s$ and $4s$, respectively, exhibiting $< 1\,\mathrm{cm}^{-1}$ splitting around $R = 1.0$ au [13].

Numerical results for BO energies obtained in this work, together with uncertainties originating purely from extrapolation to the complete basis set (CBS) limit are presented in Tables S1 – S26 in the Supplementary Material [45]. Additional quantities such as dE/dR, $-\langle\nabla_1^2\rangle/2$ and $-\langle\nabla_1 \cdot \nabla_2\rangle/2$ along with E itself are reported in raw format of the Supplementary Material [46]. Unsurprisingly, convergence for triplet states is better than for

singlet, because the requirement of antisymmetry of total fermionic wavefunction generally results in less electron-electron correlation – well-known phenomenon of *correlation hole*.

Table 1: Exemplary values of optimal nonlinear parameters for states and internuclear distances with high ionic component.

state	R	sector 1				sector 2			
		y	x	u	w	y	x	u	w
$B\,1^1\Sigma_u^+$	10.0	0.047	-0.447	0.338	0.468	-0.949	-1.263	1.052	1.226
$H\bar{H}\,4^1\Sigma_g^+$	12.0	0.000	-0.446	0.263	0.506	-0.807	-0.807	1.068	1.068
$6^1\Sigma_u^+$	15.0	0.079	-0.490	0.163	0.493	-0.863	-0.727	0.847	0.520
$7^1\Sigma_g^+$	20.0	-0.357	-0.858	0.276	0.692	-0.428	0.164	0.445	0.146

From inspection of potential curves in Figures 1 and 3 to 5, one evident universal feature for all the considered states is the presence of principal minimum around 2 bohrs. Existence of a second minimum is mainly driven by the interaction of energy levels with purely ionic H^+H^- system. A modest drop in convergence rate can be noticed for the states: $EF\,2^1\Sigma_g^+$, $H\bar{H}\,4^1\Sigma_g^+$, $7^1\Sigma_g^+$ and $B\,1^1\Sigma_u^+$, $B''\bar{B}\,3^1\Sigma_u^+$, and $6^1\Sigma_u^+$ in regions of large R, where this interaction is most prevalent and configurations mix markedly. This observation is consistent with the optimal values that nonlinear parameters attain, see Table 1 for exemplary values. For detailed analysis of ionic and covalent components we refer to Ref. [6, 7]. In Table 2 we present exemplary values of optimal nonlinear parameters for $n = 7$ states. Evident asymmetry between parameters of first and second electron justifies the use of more flexible KW basis over its more symmetric special cases. We conjecture that the same basis type can be used as a remedy for the convergence rate of ionic states if our basis is augmented with a third scale sector, improving the representation of electron correlation, when both are localized around the same nucleus, similarly as it was performed in the calculations of HeH^+[41] BO potential and recognized as a feature of *in-out* electronic correlation in one-center, two-electron calculations of He [33].

All the considered states dissociate as $H(1s) + H(nl)$ with energies tending to the sum of its dissociation products as $R \to \infty$, see Figures 1 and 3 to 5. On the other hand, in the united atom limit, $R \to 0$, electronic configuration should approach those of He. Straightforward observation that the order of energies of atomic configurations $He[^{1,3}L(1snl)]$ is in general different than corresponding $H(1s) + H(nl)$ dissociation products, together with well-known theorem that the BO potential curves with the same sym-

Table 2: Exemplary values of optimal nonlinear parameters for $n = 7$ at various internuclear distances. Notice very small values of y,u in sector 1 and x,w in sector 2, corresponding to very diffuse (high n) highly excited atomic orbitals.

state	R	sector 1				sector 2			
		y	x	u	w	y	x	u	w
$7^1\Sigma_g^+$	2.0	0.000	-0.423	0.097	0.821	-0.080	-0.122	0.637	0.262
$7^3\Sigma_g^+$	4.0	0.000	-0.405	0.097	0.638	0.080	0.278	0.624	0.114
$7^1\Sigma_u^+$	6.0	-0.061	-0.514	0.146	0.619	-0.285	0.080	0.578	0.080
$7^3\Sigma_u^+$	8.0	0.047	-0.449	0.105	0.553	0.436	0.000	0.522	0.267

metry cannot cross, implies that the character of the states must change in the region of intermediate R. The first qualitative approach aiming to predict such configuration mixing in terms of so-called correlation diagrams can be attributed to Mulliken [31], while a detailed discussion on configuration mixing and matching of Σ^+ manifolds electronic densities to the corresponding atomic orbitals was presented in the meticulous analysis by Corongiu and Clementi [6, 7, 8]. Here, we supplement this discussion with the help of Figure 2, where we present accurate splittings between singlet and triplet energies approaching the united atom configuration, including $(1snf)$ states which are split by values as small as $\sim 10^{-8}$ au.

Table 3: Comparison of calculated BO energies (hartrees) for selected states at internuclear distance of 2 bohrs (vicinity of first minimum). Long dash indicates no data available for given method. Underlined digits present an improvement over previous most accurate result.

Method	Ref.	$EF\,2^1\Sigma_g^+$	$H\bar{H}\,4^1\Sigma_u^+$	$7\,^3\Sigma_u^+$
Full CI	[6, 7, 8]	-0.717 68	-0.634 09	-0.618 97
FC-LSE	[12]	-0.717 724 7(96)	-0.634 105(21)	-0.618 207(64)
GGTOs	[9]	—	-0.634 098 15	—
ECG	[11]	-0.717 715 240	—	—
KW	[14],[16]	-0.717 715 096	-0.634 101 622 0	—
KW	this work	-0.717 715 279 148 71(3)	-0.634 101 640 058 24(1)	-0.618 969 968 931(3)

For the sake of comparison with the most recent integral-free FC-LSE calculations by Nakashima and Nakatsuji [12], we refer to the definition of H-square, see Eq. (24) of Ref. [43],

$$\sigma^2_{FC-LSE} = \langle\Psi|\,(H-E)^2\,|\Psi\rangle, \tag{10}$$

which is utilized in Ref. [12] as a measure of wavefunction (and energy)

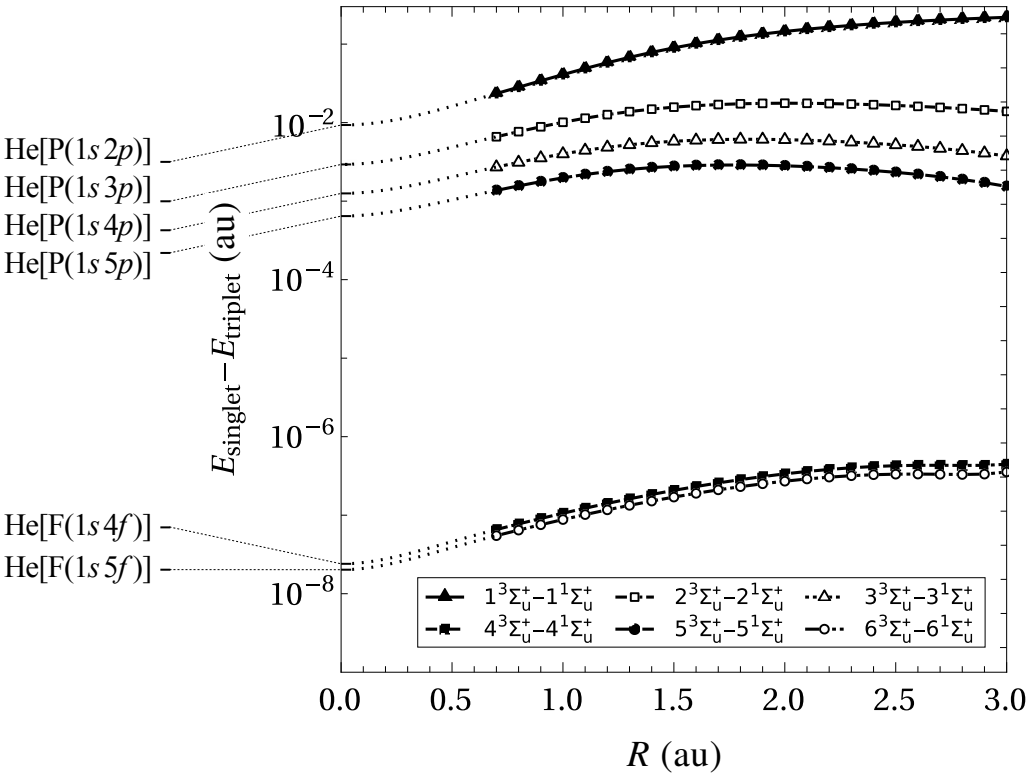

Figure 2: Energy splittings between singlet and triplet $n\,\Sigma_u^+$ states at small internuclear distances. Labels on the y axis indicate values of energy differences between helium $^1L(1snl)$ and $^3L(1snl)$ states (here with L =P,F for the states under consideration). Dotted lines represent tentative assignments from calculated splittings to corresponding differences between united atom ($R \to 0$) energies from Ref. [42], which are in agreement with [7, 8].

accuracy. For convenience, we define a relative ratio p as,

$$p = \frac{E_{var} - E_{FC-LSE}}{\sigma^2_{FC-LSE}}, \tag{11}$$

where E_{var} denotes the variational energy result as obtained in this work and E_{FC-LSE} refers to results of the FC-LSE method from Ref. [12]. One observes, that in the case of the highly excited $7^3\Sigma_u^+$ state, p is much greater than 1 for the majority of points and varies significantly (up to ~ 90) along with internuclear distance with no visible trend. In contrast, another highly excited states available for the reference, such as $6^1\Sigma_u^+$ or $7^1\Sigma_g^+$, have $p > 1$ consistently in the region $R = 2.0 - 6.0$ au. For $n > 4$ and all symmetries, systematically, more than half of the points fall outside the range of

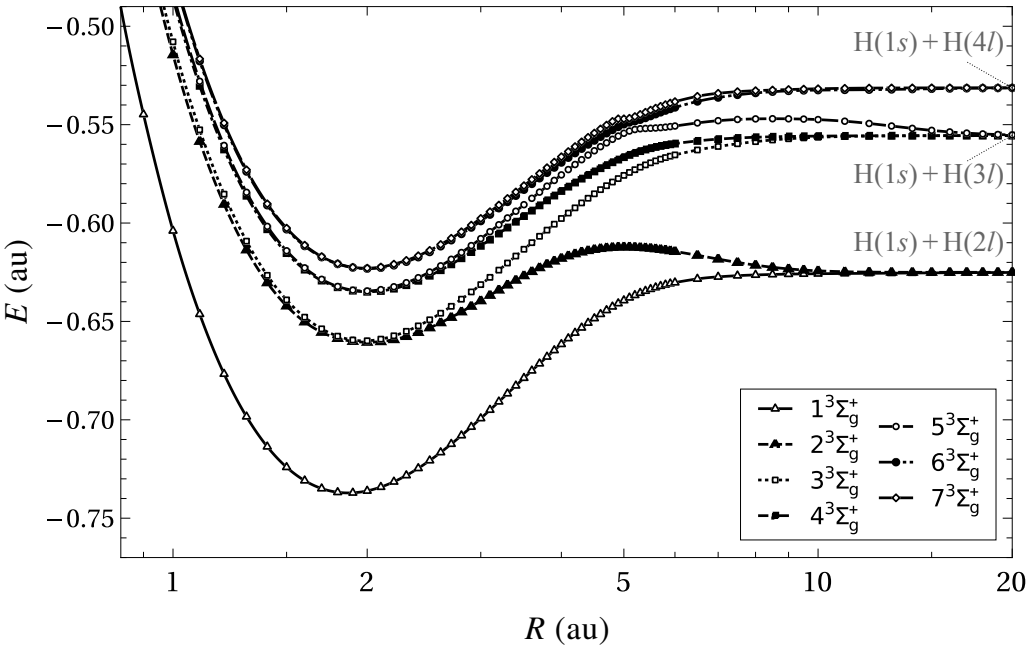

Figure 3: BO potentials for $n^3\Sigma_g^+$ states, up to $n = 7$. Pairs of states $2-3$, $4-5$ and $6-7$ all anticross around the $R = 2.0$ au minima, conjointly changing the character from united atom $3d\sigma, 4d\sigma, 5d\sigma$ to $3s, 4s, 5s$, respectively.

confidence for triplet states, if H-square is given the interpretation of 1σ confidence interval. Therefore, we conclude that H-square vastly underestimates the actual uncertainty of wavefunctions (and of energies) obtained in Ref. [12], especially in case of triplet states and for large distances. Not surprisingly, a detailed comparison in Table 3 of numerical results with their uncertainties for all the previous calculations for selected excited states at given distance of $R = 2.0$ au indicates that almost no previous calculations were able to correctly estimate numerical uncertainties.

4. Conclusions

We have demonstrated that a relative accuracy of 10^{-10} or better can be reached for BO energies of all the excited $n\,\Sigma^+$ states of H_2 up to $n = 7$, with at most 18 000 basis functions of explicitly correlated exponential basis. With a two-sector unrestricted Kolos-Wolniewicz basis, a rapid, exponential convergence towards the CBS limit is attained, even for exceptionally complicated electronic configurations of high singly-excited orbitals.

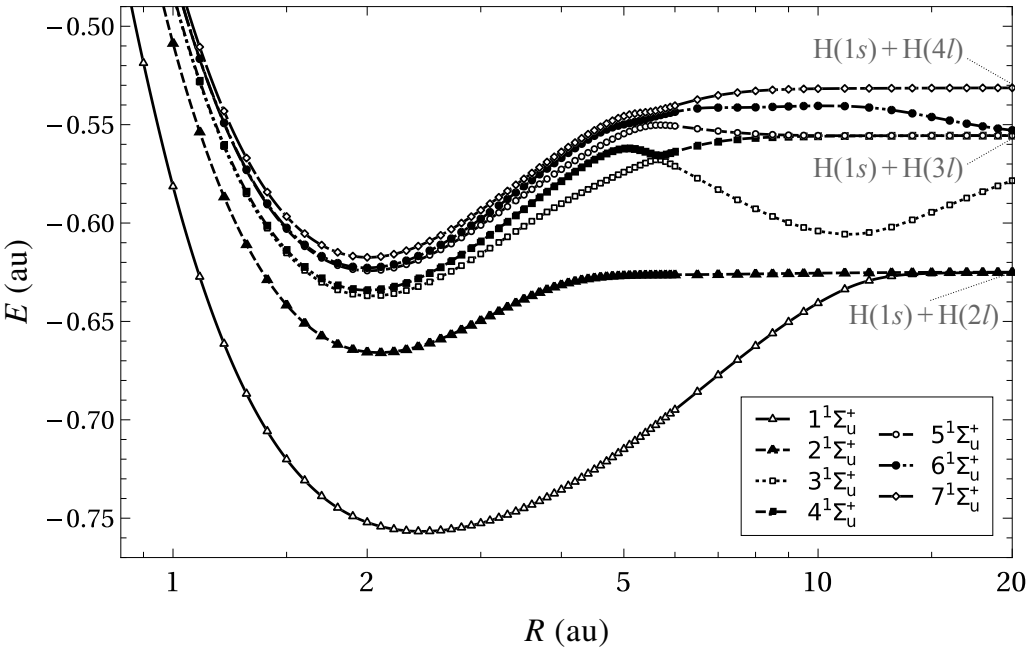

Figure 4: BO potentials for $n\,^1\Sigma_u^+$ states, up to $n = 7$.

Adiabatic corrections are known to be of significant magnitude [16] and this work paves the way towards their accurate evaluation with method similar to that presented in Ref. [44]. Ultimately, because the results obtained in this work are at least 6 orders of magnitude more accurate than any other available in the literature, we believe that they will serve as a useful benchmark for less accurate computational methods. Moreover, our two-body two-center integrals with exponential functions can be used for any two-center systems, giving the possibility of achieving high-precision results for an arbitrary diatomic molecules.

Supplementary Material

For the complete list of our numerical results we refer to Tables S1–S6 for the BO energies of the $2\,^1\Sigma_g^+ - 7\,^1\Sigma_g^+$ states, Tables S7–S13 for the BO energies of the $1\,^3\Sigma_g^+ - 7\,^3\Sigma_g^+$ states, Tables S14–S20 for the BO energies of the $1\,^1\Sigma_u^+ - 7\,^1\Sigma_u^+$ states, Tables S21–S26 for the BO energies of the $2\,^3\Sigma_u^+ - 7\,^3\Sigma_u^+$ states in the Supplementary Material [45].

In addition, dE/dR, $-\langle\nabla_1^2\rangle/2$ and $-\langle\nabla_1 \cdot \nabla_2\rangle/2$ along with energies are reported in raw text format of the Supplementary Material [46].

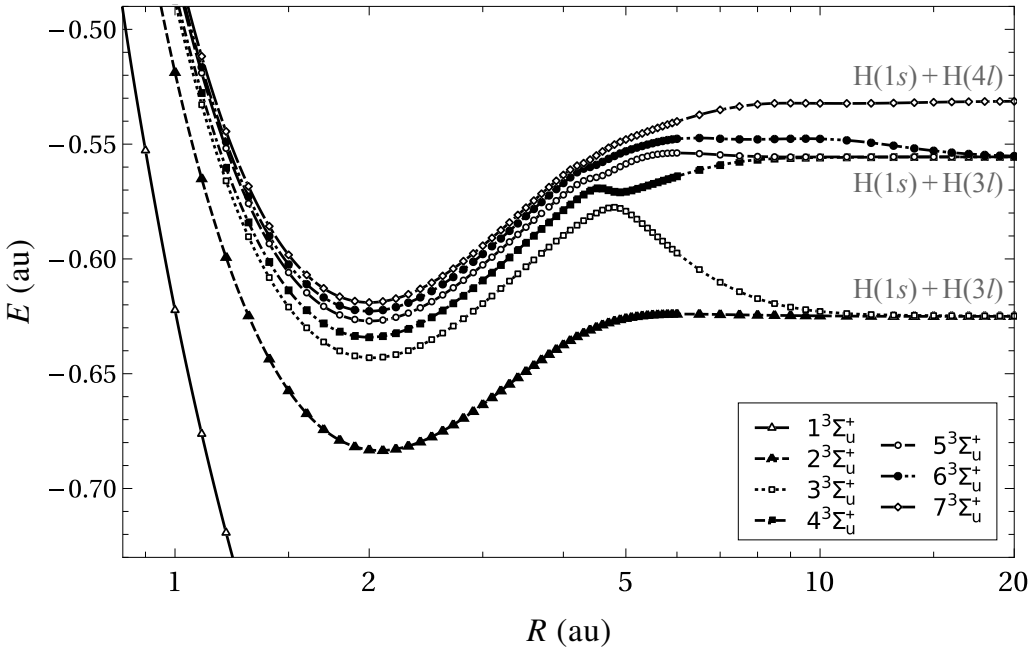

Figure 5: BO potentials for $n^3\Sigma_u^+$ states, up to $n = 7$, partial curve for $b\,1^3\Sigma_g^+$ from Ref. [30] is shown for reference.

Acknowledgement

M.S. acknowledges support from the National Science Center (Poland) under Grants No. 2020/36/T/ST2/00605 and No. 2017/27/B/ST2/02459. K.P. acknowledges support from the National Science Center (Poland) under Grant No. 2017/27/B/ST2/02459.

References

[1] Ubachs, W.; Koelemeij, J.; Eikema, K.; Salumbides, E. Physics beyond the Standard Model from hydrogen spectroscopy. *Journal of Molecular Spectroscopy* **2016**, 320, 1–12.

[2] Niu, M.; Salumbides, E.; Dickenson, G.; Eikema, K.; Ubachs, W. Precision spectroscopy of the $X\,^1\Sigma_g^+$, $\nu = 0 \rightarrow 1(J = 0$–$2)$ rovibrational splittings in H2, HD and D2. *Journal of Molecular Spectroscopy* **2014**, 300, 44–54.

[3] Lai, K.-F.; Czachorowski, P.; Schlösser, M.; Puchalski, M.; Komasa, J.; Pachucki, K.; Ubachs, W.; Salumbides, E. J. Precision tests of nonadiabatic perturbation theory with measurements on the DT molecule. *Phys. Rev. Research* **2019**, 1, 033124.

[4] Czachorowski, P.; Puchalski, M.; Komasa, J.; Pachucki, K. Nonadiabatic relativistic correction in H_2, D_2, and HD. *Phys. Rev. A* **2018**, 98, 052506.

[5] Puchalski, M.; Komasa, J.; Czachorowski, P.; Pachucki, K. Nonadiabatic QED Correction to the Dissociation Energy of the Hydrogen Molecule. *Phys. Rev. Lett.* **2019**, 122, 103003.
[6] Corongiu, G.; Clementi, E. Energy and density analyses of the H2 molecule from the united atom to dissociation: The $^1\Sigma_g^+$ states. *The Journal of Chemical Physics* **2009**, 131, 034301.
[7] Corongiu, G.; Clementi, E. Energy and Density Analyses of the $^1\Sigma_u^+$ states in the H2 Molecule from the United Atom to Dissociation. *The Journal of Physical Chemistry A* **2009**, 113, 14791–14799.
[8] Corongiu, G.; Clementi, E. Energy and density analysis of the H2 molecule from the united atom to dissociation: The $^3\Sigma_g^+$ and $^3\Sigma_u^+$ states. *The Journal of Chemical Physics* **2009**, 131, 184306.
[9] Detmer, T.; Schmelcher, P.; Cederbaum, L. S. Ab initio calculations with a nonspherical Gaussian basis set: Excited states of the hydrogen molecule. *The Journal of Chemical Physics* **1998**, 109, 9694–9700.
[10] Cencek, W.; Komasa, J.; Rychlewski, J. Benchmark calculations for two-electron systems using explicitly correlated Gaussian functions. *Chemical Physics Letters* **1995**, 246, 417–420.
[11] Komasa, J.; Cencek, W. Exponentially correlated Gaussian functions in variational calculations. The EF 1E*g state of hydrogen molecule*. *Computational Methods in Science and Technology* **2003**, 9, 79–92.
[12] Nakashima, H.; Nakatsuji, H. Solving the Schrödinger equation of hydrogen molecule with the free complement–local Schrödinger equation method: Potential energy curves of the ground and singly excited singlet and triplet states, Σ, Π, Δ, and Φ. *The Journal of Chemical Physics* **2018**, 149, 244116.
[13] Wolniewicz, L.; Dressler, K. Adiabatic potential curves and nonadiabatic coupling functions for the first five excited $^1\Sigma_g^+$ states of the hydrogen molecule. *The Journal of Chemical Physics* **1994**, 100, 444–451.
[14] Orlikowski, T.; Staszewska, G.; Wolniewicz, L. Long range adiabatic potentials and scattering lengths for the EF, eandhstates of the hydrogen molecule. *Molecular Physics* **1999**, 96, 1445–1448.
[15] Staszewska, G.; Wolniewicz, L. Transition Moments among $^3\Sigma$ and $^3\Pi$ States of the H2 Molecule. *Journal of Molecular Spectroscopy* **1999**, 198, 416–420.
[16] Staszewska, G.; Wolniewicz, L. Adiabatic Energies of Excited $^1\Sigma_u$ States of the Hydrogen Molecule. *Journal of Molecular Spectroscopy* **2002**, 212, 208–212.
[17] Wolniewicz, L.; Staszewska, G. Excited states and the transition moments of the hydrogen molecule. *Journal of Molecular Spectroscopy* **2003**, 220, 45–51.
[18] Lai, K.-F.; Beyer, M.; Salumbides, E. J.; Ubachs, W. Photolysis Production and Spectroscopic Investigation of the Highest Vibrational States in H2 (X $^1\Sigma_g^+$ $\nu = 13$, 14). *The Journal of Physical Chemistry A* **2021**, 125, 1221–1228.
[19] Sprecher, D.; Beyer, M.; Merkt, F. Precision measurement of the ionisation energy of the 3dσGK state of H2. *Molecular Physics* **2013**, 111, 2100–2107.
[20] Kouchi, N.; Ukai, M.; Hatano, Y. Dissociation dynamics of superexcited molecular hydrogen. *Journal of Physics B: Atomic, Molecular and Optical Physics* **1997**, 30, 2319–2344.
[21] Glass-Maujean, M.; Jungen, C.; Vasserot, A.; Schmoranzer, H.; Knie, A.; Kübler, S.;

Ehresmann, A.; Ubachs, W. Experimental and theoretical studies of the npσ $^1\Sigma_u^+$ and npπ $^1\Pi_u^+$ (n≥4,N$\prime$=1–6) states of D2: Energies, natural widths, absorption line intensities, and dynamics. *Journal of Molecular Spectroscopy* **2017**, 338, 22–71.

[22] Beyer, M.; Hölsch, N.; Hussels, J.; Cheng, C.-F.; Salumbides, E. J.; Eikema, K. S. E.; Ubachs, W.; Jungen, C.; Merkt, F. Determination of the Interval between the Ground States of Para- and Ortho-H_2. *Phys. Rev. Lett.* **2019**, 123, 163002.

[23] Sprecher, D.; Merkt, F. Observation of g/u-symmetry mixing in the high-n Rydberg states of HD. *The Journal of Chemical Physics* **2014**, 140, 124313.

[24] Takahashi, K.; Sakata, Y.; Hino, Y.; Sakai, Y. Doubly excited states of molecular hydrogen by scattered electron-ion coincidence measurements. *The European Physical Journal D* **2014**, 68, 83.

[25] Glass-Maujean, M. Photodissociation of doubly excited states of H2, HD, and D2. *The Journal of Chemical Physics* **1986**, 85, 4830–4834.

[26] Edwards, A. K.; Zheng, Q. Excitation of the $Q_1\,^1\Sigma_g^+$ doubly excited state of H2 by electron impact. *Journal of Physics B: Atomic, Molecular and Optical Physics* **2001**, 34, 1539–1548.

[27] Pachucki, K. Efficient approach to two-center exponential integrals with applications to excited states of molecular hydrogen. *Physical Review A* **2013**, 88, 022507.

[28] Kołos, W.; Wolniewicz, L. Potential-Energy Curve for the B $^1\Sigma_u^+$ State of the Hydrogen Molecule. *The Journal of Chemical Physics* **1966**, 45, 509–514.

[29] Pachucki, K. Born-Oppenheimer potential for H2. *Physical Review A* **2010**, 82, 032509.

[30] Pachucki, K.; Komasa, J. Gerade-ungerade mixing in the hydrogen molecule. *Physical Review A* **2011**, 83, 042510.

[31] Mulliken, R. S. The Rydberg States of Molecules. VI. Potential Curves and Dissociation Behavior of (Rydberg and Other) Diatomic States. *Journal of the American Chemical Society* **1966**, 88, 1849–1861.

[32] Sims, J. S.; Hagstrom, S. A. High precision variational calculations for the Born-Oppenheimer energies of the ground state of the hydrogen molecule. *The Journal of Chemical Physics* **2006**, 124, 094101.

[33] Drake, G. W. F. High Precision Theory of Atomic Helium. *Physica Scripta* **1999**, T83, 83.

[34] Rychlewski, J., Ed. *Explicitly Correlated Wave Functions in Chemistry and Physics*; Springer Netherlands, 2003.

[35] Pachucki, K. Correlated exponential functions in high-precision calculations for diatomic molecules. *Physical Review A* **2012**, 86, 052514.

[36] Lesiuk, M.; Moszynski, R. Analytical two-center integrals over Slater geminal functions. *Physical Review A* **2012**, 86, 052513.

[37] Aasen, J. O. On the reduction of a symmetric matrix to tridiagonal form. *BIT* **1971**, 11, 233–242.

[38] Ballard, G.; Becker, D.; Demmel, J.; Dongarra, J.; Druinsky, A.; Peled, I.; Schwartz, O.; Toledo, S.; Yamazaki, I. Implementing a Blocked Aasen's Algorithm with a Dynamic Scheduler on Multicore Architectures. 2013 IEEE 27th International Symposium on Parallel and Distributed Processing. 2013.

[39] Dongarra, J.; Gates, M.; Haidar, A.; Kurzak, J.; Luszczek, P.; Wu, P.; Yamazaki, I.; Yarkhan, A.; Abalenkovs, M.; Bagherpour, N.; Hammarling, S.;

Šístek, J.; Stevens, D.; Zounon, M.; Relton, S. D. PLASMA. *ACM Transactions on Mathematical Software* **2019**, 45, 1–35.
[40] Hida, Y.; Li, X.; Bailey, D. Algorithms for quad-double precision floating point arithmetic. Proceedings 15th IEEE Symposium on Computer Arithmetic. ARITH-15 2001. 2001.
[41] Pachucki, K. Born-Oppenheimer potential for HeH+. *Physical Review A* **2012**, 85, 042511.
[42] Drake, G. *Springer Handbook of Atomic, Molecular, and Optical Physics*; Springer New York, 2006; pp 199–219.
[43] Nakatsuji, H.; Nakashima, H. Free-complement local-Schrödinger-equation method for solving the Schrödinger equation of atoms and molecules: Basic theories and features. *The Journal of Chemical Physics* **2015**, 142, 084117.
[44] Pachucki, K.; Komasa, J. Accurate adiabatic correction in the hydrogen molecule. *The Journal of Chemical Physics* **2014**, 141, 224103.
[45] Supplementary Material in the pdf format.
[46] Supplementary Material in the plain text format.